applied sciences

MDPI

Article

Efficient Reduction in the Annual Investment Costs in AC Distribution Networks via Optimal Integration of Solar PV Sources Using the Newton Metaheuristic Algorithm

Oscar Danilo Montoya [1,2,*], Luis Fernando Grisales-Noreña [3], Lázaro Alvarado-Barrios [4,*], Andres Arias-Londoño [5] and Cesar Álvarez-Arroyo [6]

1 Facultad de Ingeniería, Universidad Distrital Francisco José de Caldas, Bogotá 110231, Colombia
2 Laboratorio Inteligente de Energía, Universidad Tecnológica de Bolívar, Cartagena 131001, Colombia
3 Department of Electromechanical and Mechatronic, Faculty of Engineering, Robledo Campus, Instituto Tecnológico Metropolitano, Medellín 050036, Colombia; luisgrisales@itm.edu.co
4 Department of Engineering, Universidad Loyola Andalucía, 41704 Sevilla, Spain
5 Facultad de Ingeniería, Campus Robledo, Institución Universitaria Pascual Bravo, Medellín 050036, Colombia; andres.arias366@pascualbravo.edu.co
6 Department of Electrical Engineering, Universidad de Sevilla, 41092 Sevilla, Spain; cesaralvarez@us.es
* Correspondence: odmontoyag@udistrital.edu.co (O.D.M.); lalvarado@uloyola.es (L.A.-B.)

Citation: Montoya, O.D.; Grisales-Noreña, L.F.; Alvarado-Barrios, L.; Arias-Londoño, A.; Álvarez-Arroyo, C. Efficient Reduction in the Annual Investment Costs in AC Distribution Networks via Optimal Integration of Solar PV Sources Using the Newton Metaheuristic Algorithm. *Appl. Sci.* **2021**, *11*, 11525. https://doi.org/10.3390/app112311525

Academic Editor: Isabel Santiago Chiquero

Received: 12 November 2021
Accepted: 1 December 2021
Published: 5 December 2021

Abstract: This research addresses the problem of the optimal placement and sizing of (PV) sources in medium voltage distribution grids through the application of the recently developed Newton metaheuristic optimization algorithm (NMA). The studied problem is formulated through a mixed-integer nonlinear programming model where the binary variables regard the installation of a PV source in a particular node, and the continuous variables are associated with power generations as well as the voltage magnitudes and angles, among others. To improve the performance of the NMA, we propose the implementation of a discrete–continuous codification where the discrete component deals with the location problem and the continuous component works with the sizing problem of the PV sources. The main advantage of the NMA is that it works based on the first and second derivatives of the fitness function considering an evolution formula that contains its current solution (x_i^t) and the best current solution (x_{best}), where the former one allows location exploitation and the latter allows the global exploration of the solution space. To evaluate the fitness function and its derivatives, the successive approximation power flow method was implemented, which became the proposed solution strategy in a master–slave optimizer, where the master stage is governed by the NMA and the slave stage corresponds to the power flow method. Numerical results in the IEEE 34- and IEEE 85-bus systems show the effectiveness of the proposed optimization approach to minimize the total annual operative costs of the network when compared to the classical Chu and Beasley genetic algorithm and the MINLP solvers available in the general algebraic modeling system with reductions of 26.89% and 27.60% for each test feeder with respect to the benchmark cases.

Keywords: placement and sizing of PV generation; AC distribution networks; Newton metaheuristic algorithm; radial distribution networks

1. Introduction

Electrical distribution networks cover hundreds of kilometers around urban and rural areas in medium- and low-voltage levels to provide electrical energy services to all end users (i.e., residential, commercial, and industrial users) [1]. The main characteristic of these networks is that these are built up in a radial configuration to reduce the investment costs of protection schemes and additional conductors [2]; however, this feature significantly increases the number of power losses in all conductors of the network since the active and reactive power travels along the grid from the substation to all the load terminals [3]. To reduce the annual operating costs of a distribution network (urban or rural), typical

solutions based on reactive power compensation [4]; grid reconfiguration schemes [5]; or shunt active power compensation with unity power factor [6]; and with variable power factor [7] are commonly found in the specialized literature. However, due to the increasing interest in the inclusion of renewable energy resources at medium- and low-voltage levels, the problem of optimal power losses reduction, although an important problem, passes to a second plane for utilities, since the main advantage of using renewables is to reduce the amount of electrical energy purchased from the conventional power system (i.e., hydro-thermal power systems) for distribution networks interconnected with the main transmission network [8]; or the number of diesel gallons in the case of isolated distribution networks [9], in addition to improving the grid efficiency in hybrid systems [10]. In addition, the increasing usage of PV sources was also promoted by the reduction in PV cells due to the advances in power electronics and generation materials such as silicon, perovskite and tandem solar cells, as presented in [11].

An important study prior to the optimal placement and sizing of PV sources in electrical networks is to explore the potential construction sites for objects that might cause shading, including high-voltage transmission towers, whose shading effects can be significant due to their height since these natural or artificial obstacles can significantly reduce the expected efficiency of the PV generation system. All of these aspects were carefully analyzed by the authors of [12].

In the specialized literature, multiple approaches focused on the optimal integration of renewable energy in distribution levels were proposed, some of which are discussed below: the authors of [13] presented the application of the recently developed vortex search algorithm to locate and estimate the size of solar photovoltaic (PV) sources in distribution networks. The classical IEEE 33- and 69-node test feeders were employed to validate their numerical results, which were compared with the mixed-integer nonlinear solvers available in the GAMS software. Numerical results demonstrated the effectiveness of the proposed methodology; however, the authors focused their attention on the reduction in the number of electrical energy losses for a typical operative day which can be an unrealistic approach due to the final costs of PV sources that are not covered by the reduction in the total cost regarding energy losses. In [14,15] Gil-González et al. have presented two approaches for integrating renewable generation based on wind and solar power in distribution networks. The main contribution of the authors of these studies is the possibility of generating reactive power with the power electronic converters that becomes the interface of the renewable generators with the power system. The exact mixed-integer nonlinear programming (MINLP) models that represent the studied problems were solved with the nonlinear solvers available in the GAMS software; even if numerical results demonstrate the advantage of including reactive power capabilities in the final objective function value with respect to the unitary power factor case, the authors did not consider economical aspects in the objective function, which in some cases, caused large renewable generation sizes that were not economically viable to the grid operator only considering the costs of the energy losses as the recovering investment factor. The authors in [16] presented a heuristic-based optimization approach based on the hybridization of the mixed-integer linear programming model with the classical simulated annealing method to solve the problem of the optimal selection and location of battery energy storage systems and PV sources in medium- and low-voltage distribution networks. The simulated annealing algorithm was used to define the type and location of the distributed energy resources along with the distribution network; while the exact mixed-integer programming was used to define their optimal daily operation. The main contribution of this research corresponds to the inclusion in the objective function of the investment and operating costs in the network presented using annualized costs. However, the main weakness of this approach is that the sizes of the PV sources and the batteries were previously set which implies that the problem becomes the optimal sizing of these devices into a selection problem, which makes their optimal solutions be highly conditioned by the initial setting of the studied devices. The authors of [8] applied the classical particle swarm optimization

method to simultaneously locate battery energy storage systems and renewable energy in electrical distribution networks. The main contribution of the authors is the economic analysis introduced considering installation, operation, and maintenance costs; however, the authors oversimplified the distribution grid, which reduces the complexity of the MINLP model to a mixed-integer linear programming model. Even if it guarantees optimal solutions for the unique nodal representation; it do not represent to the optimal solution when the grid topology is included since the problem of the optimal location (nodes' selection) is neglected. The authors in [8] proposed a new multiobjective algorithm to determine the optimal sizing and allocation of PV systems in radial distribution systems. The Jaya algorithm was modified to find the optimal PV capacities for limited bus locations in the network. The proposed algorithm showed better performance against known techniques, and the results were presented. However, the main problem with this research corresponds to the feasibility of the final solution regarding investment and operating costs since these were not considered in the optimization model.

Unlike in previously reported works, this research studies the problem of the optimal sizing and locating of PV sources in AC distribution networks operating at medium-voltage levels, considering the annualized investment and operating costs of the PV sources summed with the total energy purchasing costs at the substation bus. The main contributions of our research were the following: (i) the application of a recently developed metaheuristic optimization algorithm named the Newton metaheuristic algorithm (NMA) with a mixed discrete–continuous codification that allows defining the set of nodes where the PV sources will be located as well as their optimal sizes [17]. The proposed optimization scheme is based on the master–slave approach, where the master stage is the NMA and the slave approach corresponds to a classical power flow method for AC distribution grids. It is important to highlight that the NMA method has not previously been reported to analyze electrical networks, which was an opportunity for research that this paper tried to fulfill; and (ii) the comparison with the classical Chu and Beasley genetic algorithm using the same discrete continuous codification and the exact MINLP implementation in the general algebraic modeling system (GAMS) for two classical well-known distribution grids which are the IEEE 34- and IEEE 85-bus test feeders.

The remainder of this document is organized as follows: Section 2 presents the complete mathematical optimization model that describes the problem of the optimal placement and location of PV sources considering an economic objective function indicator based on the investments in PV sources and energy purchasing costs at the substation bus; Section 3 presents the theoretical derivation of the Newton metaheuristic optimization algorithm to solve combinatorial problems; Section 4 shows the main characteristics of the IEEE 34- and IEEE 85-node test feeders including their branch and load parameters as well as the daily behaviors of the demand at the substation terminal and the PV generation profile; Section 5 describes all the numerical validations and comparisons of the proposed NMA with the classical Chu and Beasley genetic algorithm and the BONMIN solver available in GAMS software. Finally, Section 6 presents the main concluding remarks derived from this work as some possible future research avenues.

2. Mathematical Formulation

The optimal integration of PV sources in electrical systems generates a mixed-integer nonlinear programming model due to the presence of binary variables regarding the optimal location of dispersed generators which are also combined with continuous variables regarding power flows through the network and voltage variables in all the nodes of the system [18]. The formulation of the exact MINLP model is presented below.

2.1. Objective Function Formulation

The problem of the optimal locating and sizing of PV sources in AC networks is formulated from an economical point of view. The main idea is to minimize the investment and maintenance costs of the PV sources summed with the total energy purchasing costs

in the substation bus [16]. The objective function and its components are presented in Equations (1)–(3), respectively:

$$A_{\text{cost}} = z_1 + z_2, \tag{1}$$

$$z_1 = C_{\text{kWh}} T \left(\frac{t_a}{1-(1+t_a)^{-N_t}} \right) \left(\sum_{h \in \mathcal{H}} \sum_{i \in \mathcal{N}} p_{i,h}^{cg} \Delta h \right) \left(\sum_{t_y \in \mathcal{T}} \left(\frac{1+t_e}{1+t_a} \right)_y^t \right), \tag{2}$$

$$z_2 = C_{\text{PV}} \left(\frac{t_a}{1-(1+t_a)^{-N_t}} \right) \left(\sum_{i \in \mathcal{N}} p_i^{pv} \right) + C_{O\&M} T \sum_{i \in \mathcal{N}} \sum_{h \in \mathcal{H}} p_i^{pv} G_h^{pv} \Delta h, \tag{3}$$

where A_{cost} represents the total annual operative cost of the network; z_1 is the component of the objective function regarding the expected annualized energy purchasing costs in the substation buses; z_2 is the component of the objective function regarding the investment costs in PV sources summed with their maintenance and operation costs. C_{kWh} is the average energy purchasing costs in the substation bus; T represents the number of days in an ordinary year (i.e., 365 days); t_a corresponds to the internal return rate expected for the investments made by the utility during the duration of the project; N_t is the total number of periods of the planning project in years; $p_{i,h}^{cg}$ is the active power generation output at each conventional generator connected to node i during the period of time h; Δh is the length of the period of time where the electrical variables are assumed to be constants; t_e is the average expected percentage of increment in the energy purchasing cost during the planning horizon. C_{PV} represents the average costs of installing a kW of PV power; p_i^{pv} is the size of a PV source connected to node i; $C_{O\&M}$ is the maintenance and operating costs of a PV source; and G_h^{pv} is the expected PV generation curve in the area of influence of the distribution network. Note that $\mathcal{H}$, $\mathcal{N}$, and $\mathcal{T}$ are the sets that contain all the periods of time in a daily operation scenario, the nodes of the network; and the number of years of the planning period, respectively.

2.2. Set of Constraints

The set of constraints in the problem of the optimal placement and sizing of PV sources in grid-connected distribution networks includes active and reactive power balance constraints, voltage regulation bounds, and devices capabilities, among other constraints [19]. The complete list of constraints is listed from Equations (4)–(11) [6]:

$$p_{i,h}^{cg} + p_i^{pv} G_h^{pv} - P_{i,h}^{d} = v_{i,h} \sum_{j \in \mathcal{N}} Y_{ij} v_{j,h} \cos\left(\theta_{i,h} - \theta_{j,h} - \varphi_{ij}\right), \ \{\forall i \in \mathcal{N}, \ \forall h \in \mathcal{H}\}, \tag{4}$$

$$q_{i,h}^{cg} - Q_{i,h}^{d} = v_{i,h} \sum_{j \in \mathcal{N}} Y_{ij} v_{j,h} \sin\left(\theta_{i,h} - \theta_{j,h} - \varphi_{ij}\right), \ \{\forall i \in \mathcal{N}, \ \forall h \in \mathcal{H}\}, \tag{5}$$

$$p_i^{cg,\min} \leq p_{i,h}^{cg} \leq p_i^{cg,\max}, \ \{\forall i \in \mathcal{N}, \ \forall h \in \mathcal{H}\} \tag{6}$$

$$q_i^{cg,\min} \leq q_{i,h}^{cg} \leq q_i^{cg,\max}, \ \{\forall i \in \mathcal{N}, \ \forall h \in \mathcal{H}\} \tag{7}$$

$$x_i p_i^{pv,\min} \leq p_i^{pv} \leq x_i p_i^{pv,\max}, \ \{\forall i \in \mathcal{N}\}, \tag{8}$$

$$v_i^{\min} \leq v_{i,h} \leq v_i^{\max}, \ \{\forall i \in \mathcal{N}, \ \forall h \in \mathcal{H}\} \tag{9}$$

$$\sum_{i \in \mathcal{N}} x_i \leq N_{pv}^{ava}, \tag{10}$$

$$x_i \in \{0,1\}, \ \{\forall i \in \mathcal{N}\}, \tag{11}$$

where $P_{i,h}^{d}$ and $Q_{i,h}^{d}$ are the active and reactive power demands at node i during the period of time h; $q_{i,h}^{cg}$ is the reactive power injection in the conventional source connected to node i during the period of time h; $v_{i,h}$ and $v_{j,h}$ are the voltage magnitudes at nodes i and j in the period of time h, respectively; Y_{ij} is the magnitude of the admittance that relates nodes i and j which has an angle φ_{ij}; $\theta_{i,h}$ and $\theta_{j,h}$ are the voltage angle values in nodes

i and j during each period of time; $p_i^{cg,\min}$ and $p_i^{cg,\max}$ are the active generation bounds associated with the conventional generator connected to node i; and $q_i^{cg,\min}$ and $q_i^{cg,\max}$ are the corresponding reactive power generation bounds, respectively. x_i is the binary variable associated with the installation ($x_i = 1$) or not ($x_i = 0$) of a PV source at node i; $p_i^{pv,\min}$ and $p_i^{pv,\max}$ are the minimum and maximum sizes allowed for the PV integration in the distribution grid. $\underline{v}_i^{\min}$ and $\overline{v}_i^{\max}$ represent the minimum and maximum voltage regulation bounds allowed at node i; and N_{pv}^{ava} is a constant parameter associated with the maximum number of PV sources available for installation along with the distribution grid.

2.3. Model Interpretation

The interpretation of the MINLP model defined from (1) to (11) is the following: Equation (1) defines the objective function of the optimization problem which adds the energy purchasing costs to the conventional generators (i.e., substation buses) as defined in Equation (2) with the annualized investments in PV sources including its maintenance and operating costs as defined by Equation (3). Equality constraints (4) and (5) present the active and reactive power equilibrium at each node of the system for each period of time. These equations are the most complex constraints in the studied problem since these are nonlinear, non-convex, and typically require numerical methods to be properly addressed. Box-type constraints (6) and (7) define the lower and upper bounds associated with the active and reactive power generation outputs in the conventional sources; the Box-type constraint (9) defines the PV lower and upper generation capabilities for the PV sources in case that the binary variable is activated; the Box-type constraint (10) presents the lower and upper voltage regulation limits allowed for all nodes of the network. This is a typical constraint imposed by regulatory entities and utility operation practices. The inequality constraint (10) limits the maximum number of PV sources that can be installed along with the distribution network; finally, constraint (11) shows the binary nature of the decision variable regarding whether or not to locate a PV source in a particular node of the network.

It is worth mentioning that the main complication of the optimization model (1)–(11) is its MINLP nature, since binary and continuous variables are combined with nonlinear non-convex relations mainly defined by the power balance equations. To solve MINLP models, in the current literature, the use of master–slave optimization strategies is a popular method to decouple the binary problem from the continuous problem [20]. In the studied problem defined by (1)–(11), the Newton metaheuristic algorithm is used in the master stage and the successive approximation power flow method is used in the slave stage.

3. Methodology of Solution

To solve the complex MINLP model defined by (1)–(11) in this research, we adopted a recently developed combinatorial optimization method named the Newton metaheuristic algorithm which was originally proposed in [21] to solve a discrete optimization problem regarding the optimal design of steel structures. Here, the NMA is used as the master optimization stage to define the optimal placements and sizes of the PV sources in the AC distribution network by using a discrete–continuous codification with the form presented in (12) [13]:

$$x_j^t = \left[2,\ k,\ldots,\ n \mid p_2^{pv},\ p_k^{pv},\ \ldots,\ p_n^{pv}\right], \tag{12}$$

where x_j^t is the solution of individual j at iteration t; in addition, the dimension of this vector is $1 \times 2N_{pv}^{ava}$ and the first N_{pv}^{ava} is associated with the nodes where the PV sources will be installed (discrete part of the codification), while its second part is regards their optimal sizes (continuous part of the codification). The main idea of the NMA is to evolve the initial population through the solution space by using the same ideas of the Newton algorithm to solve sets of nonlinear equations and find their roots.

3.1. Master Stage

The general evolution rule to solve a nonlinear equation $f(x) = 0$ by starting from the initial point x_j^0 with the Newton's method takes the structure reported in Equation (13) [21]:

$$x_j^{t+1} = x_j^t - \frac{f\left(x_j^t\right)}{f'\left(x_j^t\right)}, \tag{13}$$

where $f'\left(x_j^t\right)$ is the derivative of the function evaluated at point x_j^t. The main advantage of this iterative algorithm is that its convergence is quadratic, which implies that in a few iterations, the searched solution can be found; however, when we try to apply this rule to an optimization problem, where the objective is to find a local (or global) minimum/maximum, we know that $f'\left(x_j^t\right) = 0$. This also implies that the evolution rule (13) is undefined. To deal with this problem, the authors of [21], proposed the application of the Newton evolution rule to the derivative of the function $f\left(x_j^t\right)$, i.e., $f'\left(x_j^t\right)$, that produces a modified evolution rule defined in (14).

$$x_j^{t+1} = x_j^t - \frac{f'\left(x_j^t\right)}{f''\left(x_j^t\right)}, \tag{14}$$

where the main challenge is to determine the values of the functions $f'\left(x_j^t\right)$ and $f''\left(x_j^t\right)$ as a function of the known value of $f\left(x_j^t\right)$. Note that the value of the $f\left(x_j^t\right)$ at each individual x_j^t will be provided by the solution of the power flow problem in the slave stage that will be subsequently explained herein.

To obtain the value of the derivatives $f'\left(x_j^t\right)$ and $f''\left(x_j^t\right)$, we considered that the distance of the previous and the following solutions with respect to x_j^t taking the form presented in Equations (15) and (16) [21]:

$$x_j^t - x_{j-1}^t = \tau\left(x_{j+1}^t - x_{j-1}^t\right), \tag{15}$$

$$x_{j+1}^t - x_j^t = (1-\tau)\left(x_{j+1}^t - x_{j-1}^t\right), \tag{16}$$

where τ is a positive parameter.

To obtain a relation between function $f(x)$ and its first and second derivatives, the Taylor's series expansion was applied, considering its first two terms, which produced the relation defined in Equation (17):

$$f(x) = f\left(x_j^t\right) + \left(x - x_j^t\right)f'\left(x_j^t\right) + \frac{\left(x - x_j^t\right)^2}{2}f''\left(x_j^t\right). \tag{17}$$

Now, if we define λ as $x_{j+1}^t - x_{j-1}^t$, and we also combine Equations (14)–(16), then the function values at points x_{j+1}^t and x_{j-1}^t can be obtained as presented in Equations (18) and (19):

$$f\left(x_{j+1}^t\right) = f\left(x_j^t\right) + \lambda(1-\tau)f'\left(x_j^t\right) + \frac{\lambda^2(1-\tau)^2}{2}f''\left(x_j^t\right). \tag{18}$$

$$f\left(x_{j-1}^t\right) = f\left(x_j^t\right) - \lambda\tau f'\left(x_j^t\right) + \frac{\lambda^2\tau^2}{2}f''\left(x_j^t\right). \tag{19}$$

Simultaneously, solving Equations (18) and (19) for $f'\left(x_i^t\right)$ and $f''\left(x_i^t\right)$ yields Equations (20) and (21):

$$f'\left(x_j^t\right) = \frac{\tau^2 f\left(x_{j+1}^t\right) + (1-2\tau) f\left(x_j^t\right) - (1-\tau)^2 f\left(x_{j-1}^t\right)}{\tau(1-\tau)\left(x_{j+1}^t - x_{j-1}^t\right)}. \tag{20}$$

$$f''\left(x_j^t\right) = \frac{2\tau f\left(x_{j+1}^t\right) - 2f\left(x_j^t\right) + 2(1-\tau) f\left(x_{j-1}^t\right)}{\tau(1-\tau)\left(x_{j+1}^t - x_{j-1}^t\right)^2}. \tag{21}$$

By combining Equations (20) and (21) in Equation (14), the evolution rule of the Newton metaheuristic algorithm takes the form defined in Equation (22):

$$x_j^{t+1} = x_j^t + \frac{\tau^2 f\left(x_{j+1}^t\right) + (1-2\tau) f\left(x_j^t\right) - (1-\tau)^2 f\left(x_{j-1}^t\right)}{2\tau f\left(x_{j+1}^t\right) - 2f\left(x_j^t\right) + 2(1-\tau) f\left(x_{j-1}^t\right)}\left(x_{j-1}^t - x_{j+1}^t\right). \tag{22}$$

Note that the evolution rule presented in (22) depends on the parameter τ which was defined as recommended in [21] as presented in Equation (23):

$$\tau = \frac{\left\| x_j^t - x_{j-1}^t \right\|}{\left\| x_{j+1}^t - x_{j-1}^t \right\|}, \tag{23}$$

Remark 1. *Based on the recommendations of the authors in [21], the evolution rule (22) can be improved by considering the position of the best optimal solution at the current iteration (i.e., x_{best}^t) which generates the evolution rule to explore and exploit the solution space that is defined in Equation (24).*

$$x_j^{t+1} = x_j^t + \frac{t}{t_{\max}} r_1 \Gamma\left(x_{j-1}^t - x_{j+1}^t\right) + \left(1 - \frac{t}{t_{\max}}\right) r_2\left(x_{best}^t - x_j^t\right), \tag{24}$$

where r_1 and r_2 are random numbers between 0 and 1, $t_{\max}$ is the maximum number of iterations, and Γ takes the form presented in Equation (25):

$$\Gamma = \frac{\tau^2 f\left(x_{j+1}^t\right) + (1-2\tau) f\left(x_j^t\right) - (1-\tau)^2 f\left(x_{j-1}^t\right)}{2\tau f\left(x_{j+1}^t\right) - 2f\left(x_j^t\right) + 2(1-\tau) f\left(x_{j-1}^t\right)}, \tag{25}$$

It is worth mentioning that the evaluation of the Γ function requires knowing the objective function values $f\left(x_{j-1}^t\right)$, $f\left(x_j^t\right)$, and $f\left(x_{j+1}^t\right)$, respectively. The evaluation of these functions were obtained through the slave stage, which is presented below.

3.2. Slave Stage

The slave optimization stage in master–slave optimization algorithms corresponds to the core (i.e., heart) of the metaheuristic since this explores and exploits the solution space [22]. In the case of the optimization applied to the electrical networks, the slave stage is typically associated with the recursive evaluation of the power flow problem for each individual x_j^t. In this research, we employ the power flow approach known as the successive approximation method initially reported in [23] for AC distribution networks, with the main advantage that its convergence can be guarantee through the application of the Banach fixed-point theorem [24].

The recursive power flow formula to solve power flow problems in AC distribution networks takes the structure presented in Equation (26) [25]:

$$\mathbb{V}_{d,h}^{m+1} = \mathbb{Y}_{dd}^{-1}\left[\mathbf{diag}^{-1}\left(\mathbb{V}_{d,h}^{\star,m}\right)\left(\mathbb{S}_{pv,h}^{\star} - \mathbb{S}_{d,h}^{\star}\right) - \mathbb{Y}_{ds}\mathbb{V}_{s,h}\right], \tag{26}$$

where m represents the counter of iterations, $\mathbb{V}_{d,h}$ is the vector that has all the voltage variables in the demand nodes in complex form (note that for $t = 0$, we consider the plane voltages, i.e., $\mathbb{V}_{d,h}^{t+1} = 1\angle 0°$). $\mathbb{Y}_{dd}$ and $\mathbb{Y}_{ds}$ are sub-components of the general nodal admittance matrix that connect the demand and slack nodes among them. $\mathbb{S}_{pv,h}^{\star}$ is a vector that contains all the complex power injections in the PV sources (where it is assumed that they are designed with unity power factor); $\mathbb{V}_{s,h}$ represents the vector with the complex voltage outputs in the slack sources (i.e., known voltage values). It is worth mentioning that the operator $\mathbf{diag}(\theta)$ transforms the vector θ into a diagonal matrix; and $\theta^{\star}$ is the complex conjugate value of the vector θ.

The recursive evaluation of the power flow formula (26) ends when the convergence error is met between two consecutive voltage iterations. This criterion is defined in (27):

$$\max\left\{\left|\left|\mathbb{V}_{d,h}^{t+1}\right| - \left|\mathbb{V}_{d,h}^{t}\right|\right|\right\} \leq \zeta, \tag{27}$$

where ζ represents the error of convergence which is assigned as 1×10^{-10} based on the recommendation of [24].

Note that the NMA sends the combination of the output powers for the PV sources with their locations to the slave stage, i.e., $\mathbb{S}_{pv}^{\star}$, which are considered inputs for the power flow formula (26). With this information, the fitness function that guides the exploration and exploitation process in the master optimization stage is calculated. Note that, to calculate the annualized energy purchasing costs at the substation buses, all the voltages provided by the solution of the power flow problem were evaluated in (28), i.e., $\mathbb{V}_{d,h}$, which allowing to compute the total slack complex power generation as defined in Equation (28).

$$\mathbb{S}_{cg,h}^{\star} = \mathbf{diag}\left(\mathbb{V}_{s,h}^{\star}\right)\left[\mathbb{Y}_{sd}\mathbb{V}_{d,h} + \mathbb{Y}_{ss}\mathbb{V}_{s,h}\right]. \tag{28}$$

The evolution through the solution space for the NMA is guided by the value of the fitness objective function value, which corresponds to the summation of the objective function of the studied problem with some penalties associated with the constraints to ensure the solutions' feasibility. The proposed fitness function is presented in Equation (29):

$$z_f = A_{\text{cost}} + \alpha_1 \max_h\left\{0, \left|\mathbb{V}_{d,h}\right| - v_{\max}\right\} - \alpha_2 \min_h\left\{0, \left|\mathbb{V}_{d,h}\right| - v_{\min}\right\} - \alpha_3 \min_h\left\{0, \text{real}\left\{\mathbb{S}_{cg,h}^{\star}\right\}\right\}, \tag{29}$$

where α_1, α_2, and α are the penalization factors associated with the violation of the voltage's regulation bounds, and the non-negativeness requirement of the power generation in the slack source, respectively. These factors generate adaptive penalty factors defined as a function of the deviation value regarding the lower and upper voltage bounds in the case of the voltages, or the magnitude of the violation of the non-negative requirement of the power output at the substation bus. It is worth mentioning that the fitness function (z_f) is equal to the objective function when all the constraints in the mathematical model (1)–(11) are met.

In the case of the upper and lower bounds of the PV generation, these are guaranteed with the proposed codification generation. In the case that one descending individual x_j^{t+1} is out of the generation bounds, this is corrected through the rule defined in Equation (30):

$$x_{j,k}^{t+1} = \begin{cases} x_{j,k}^{t+1} & : x_{j,k}^{\min} \leq x_{j,k}^{t+1} \leq x_{j,k}^{\max} \\ x_{j,k}^{t+1} & : x_{j,k}^{\min} + r\left(x_{j,k}^{\max} - x_{j,k}^{\min}\right) \end{cases} \tag{30}$$

where r is a random number between 0 and 1, and $x_{j,k}^{\min}$, and $x_{j,k}^{\max}$ are the maximum and minimum values allowed for the decision variables regarding the location and sizing of the PV sources.

3.3. General Solution Flow Chart

To summarize the main aspects of the proposed optimization approach based on the hybridization of the NMA with the successive approximation power flow method for the optimal locating and sizing of PV sources in AC distribution networks, we present the flow diagram depicted in Figure 1.

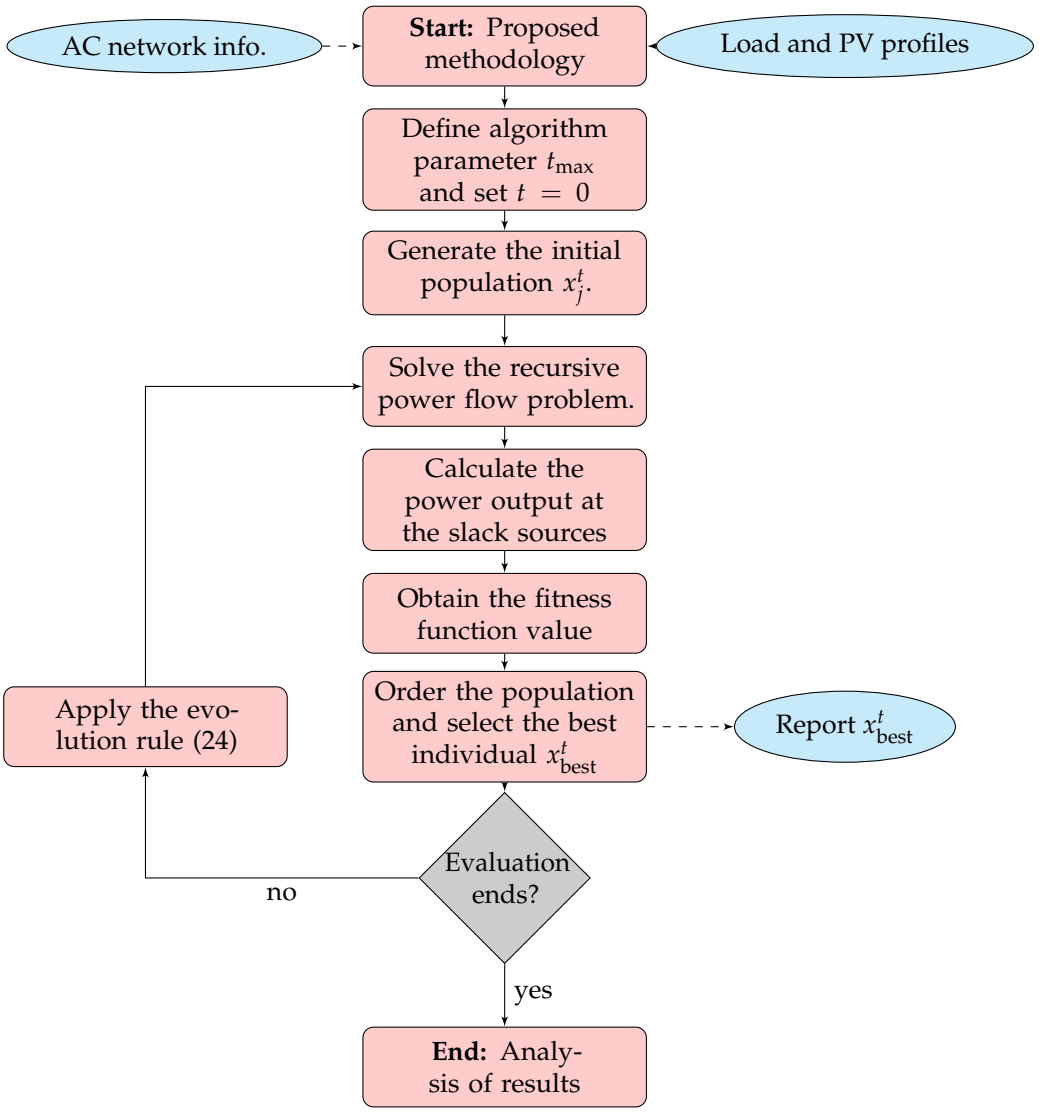

Figure 1. Implementation guide for the proposed optimization approach.

Note that the flow diagram presented in Figure 1 is general and can be applied for any combinatorial optimization technique that works in a master–slave connection with a power flow to locate and size renewable generation sources in AC distribution networks.

4. Test Feeders

To validate the effectiveness and robustness of the proposed master–slave optimization approach to locate and size PV sources based on the NMA, two test feeders composed of 34 and 85 buses were employed. The main characteristics for both test feeders are presented below.

4.1. IEEE 34-Node Test Feeder

The IEEE 34-node test feeder is an electrical distribution network comprising 34 nodes and 33 lines with radial structure, where the substation is operated at 11 kV. The interconnection among nodes for this test feeder is depicted in Figure 2 [25]. The peak power consumption in this system is $4636.50 + j2873.50$ kVA, which generates 221.75 kW and 65.12 kvar of power losses at the peak hour, respectively.

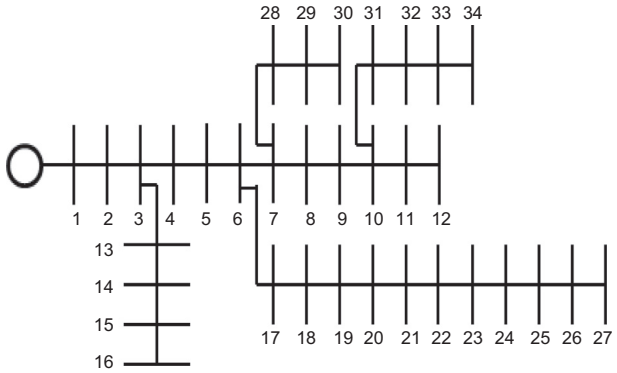

Figure 2. General interconnection among nodes in the IEEE 34-node test feeder.

The information concerning branch parameters and load consumptions for the IEEE 34-node test feeder were reported in Table 1. In all the computational validations, 11 kV and 1000 kVA were considered as voltage and power bases for this system, respectively.

Table 1. IEEE 34-node test feeder parameters.

k	m	R_{km} (Ω)	x_{km} (Ω)	P_k (kW)	Q_k (kW)	k	m	R_{km} (Ω)	x_{km} (Ω)	P_k (kW)	Q_k (kW)
1	2	0.1170	0.0480	230	142.5	18	19	0.2079	0.0473	230	142.5
2	3	0.1073	0.0440	0	0	19	20	0.1890	0.0430	230	142.5
3	4	0.1645	0.0457	230	142.5	20	21	0.1890	0.0430	230	142.5
4	5	0.1495	0.0415	230	142.5	21	22	0.2620	0.0450	230	142.5
5	6	0.1495	0.0415	0	0	22	23	0.2620	0.0450	230	142.5
6	7	0.3144	0.0540	0	0	23	24	0.3144	0.0540	230	142.5
7	8	0.2096	0.0360	230	142.5	24	25	0.2096	0.0360	230	142.5
8	9	0.3144	0.0540	230	142.5	25	26	0.1310	0.0225	230	142.5
9	10	0.2096	0.0360	0	0	26	27	0.1048	0.0180	137	85
10	11	0.1310	0.0225	230	142.5	7	28	0.1572	0.0270	75	48
11	12	0.1048	0.0180	137	84	28	29	0.1572	0.0270	75	48
3	13	0.1572	0.0270	72	45	29	30	0.1572	0.0270	75	48
13	14	0.2096	0.0360	72	45	10	31	0.1572	0.0270	57	34.5
14	15	0.1048	0.0180	72	45	31	32	0.2096	0.0360	57	34.5
15	16	0.0524	0.0090	13.5	7.5	32	33	0.1572	0.0270	57	34.5
6	17	0.1794	0.0498	230	142.5	33	34	0.1048	0.0180	57	34.5
17	18	0.1645	0.0457	230	142.5	—	—	—	—	—	—

4.2. IEEE 85-Node Test Feeder

The IEEE 85-bus system has a radial medium-voltage distribution network composed of 85 nodes and 85 lines, operated with 11 kV. The total active and reactive power demand for this system is $2570.28 + j2622.20$ kVA. The electrical configuration of this system is provided in Figure 3, and all its parametric information was taken from [26], which is given in Table 2.

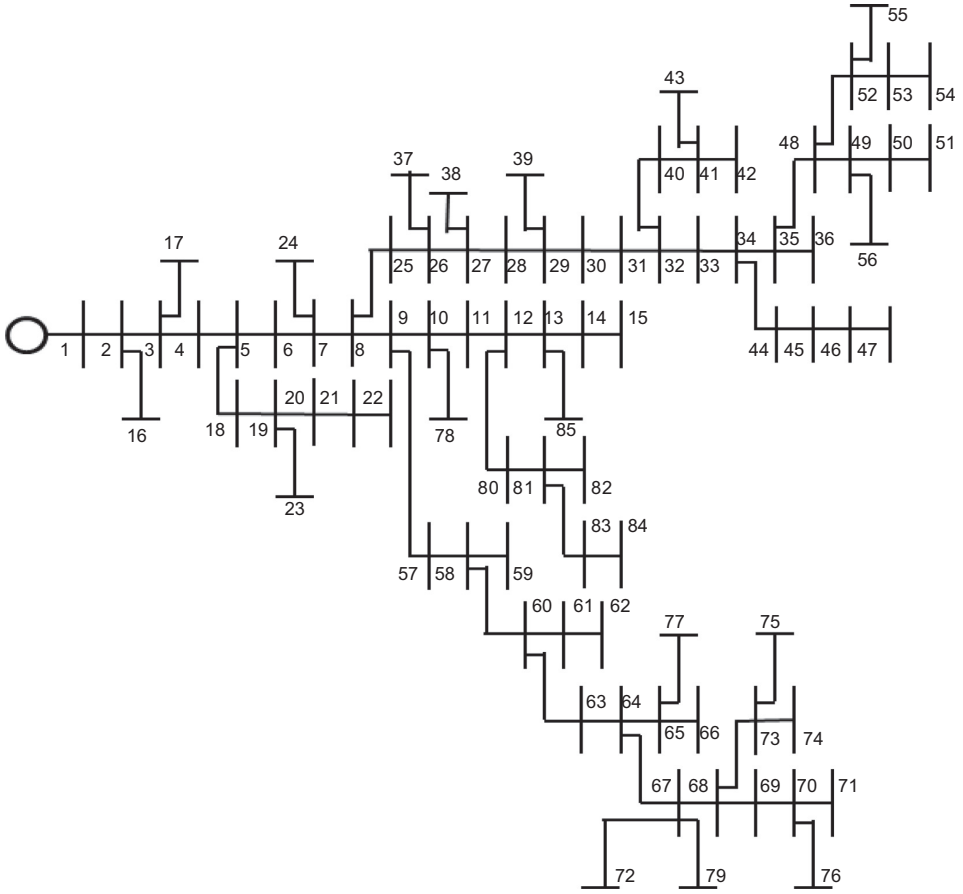

Figure 3. General interconnection among nodes in the IEEE 85-node test feeder.

Table 2. IEEE 85-node test feeder parameters

k	m	R_{km} (Ω)	x_{km} (Ω)	P_k (kW)	Q_k (kW)	k	m	R_{km} (Ω)	x_{km} (Ω)	P_k (kW)	Q_k (kW)
1	2	0.108	0.075	0	0	34	44	1.002	0.416	35.28	35.99
2	3	0.163	0.112	0	0	44	45	0.911	0.378	35.28	35.99
3	4	0.217	0.149	56	57.13	45	46	0.911	0.378	35.28	35.99
4	5	0.108	0.074	0	0	46	47	0.546	0.226	14	14.28
5	6	0.435	0.298	35.28	35.99	35	48	0.637	0.264	0	0
6	7	0.272	0.186	0	0	48	49	0.182	0.075	0	0
7	8	1.197	0.820	35.28	35.99	49	50	0.364	0.151	36.28	37.01
8	9	0.108	0.074	0	0	50	51	0.455	0.189	56	57.13
9	10	0.598	0.410	0	0	48	52	1.366	0.567	0	0
10	11	0.544	0.373	56	57.13	52	53	0.455	0.189	35.28	35.99
11	12	0.544	0.373	0	0	53	54	0.546	0.226	56	57.13
12	13	0.598	0.410	0	0	52	55	0.546	0.226	56	57.13
13	14	0.272	0.186	35.28	35.99	49	56	0.546	0.226	14	14.28
14	15	0.326	0.223	35.28	35.99	9	57	0.273	0.113	56	57.13
2	16	0.728	0.302	35.28	35.99	57	58	0.819	0.340	0	0
3	17	0.455	0.189	112	114.26	58	59	0.182	0.075	56	57.13
5	18	0.820	0.340	56	57.13	58	60	0.546	0.226	56	57.13
18	19	0.637	0.264	56	57.13	60	61	0.728	0.302	56	57.13
19	20	0.455	0.189	35.28	35.99	61	62	1.002	0.415	56	57.13
20	21	0.819	0.340	35.28	35.99	60	63	0.182	0.075	14	14.28
21	22	1.548	0.642	35.28	35.99	63	64	0.728	0.302	0	0
19	23	0.182	0.075	56	57.13	64	65	0.182	0.075	0	0
7	24	0.910	0.378	35.28	35.99	65	66	0.182	0.075	56	57.13
8	25	0.455	0.189	35.28	35.99	64	67	0.455	0.189	0	0
25	26	0.364	0.151	56	57.13	67	68	0.910	0.378	0	0
26	27	0.546	0.226	0	0	68	69	1.092	0.453	56	57.13
27	28	0.273	0.113	56	57.13	69	70	0.455	0.189	0	0

Table 2. *Cont.*

k	m	R_{km} (Ω)	x_{km} (Ω)	P_k (kW)	Q_k (kW)	k	m	R_{km} (Ω)	x_{km} (Ω)	P_k (kW)	Q_k (kW)
28	29	0.546	0.226	0	0	70	71	0.546	0.226	35.28	35.99
29	30	0.546	0.226	35.28	35.99	67	72	0.182	0.075	56	57.13
30	31	0.273	0.113	35.28	35.99	68	73	1.184	0.491	0	0
31	32	0.182	0.075	0	0	73	74	0.273	0.113	56	57.13
32	33	0.182	0.075	14	14.28	73	75	1.002	0.416	35.28	35.99
33	34	0.819	0.340	0	0	70	76	0.546	0.226	56	57.13
34	35	0.637	0.264	0	0	65	77	0.091	0.037	14	14.28
35	36	0.182	0.075	35.28	35.99	10	78	0.637	0.264	56	57.13
26	37	0.364	0.151	56	57.13	67	79	0.546	0.226	35.28	35.99
27	38	1.002	0.416	56	57.13	12	80	0.728	0.302	56	57.13
29	39	0.546	0.226	56	57.13	80	81	0.364	0.151	0	0
32	40	0.455	0.189	35.28	35.99	81	82	0.091	0.037	56	57.13
40	41	1.002	0.416	0	0	81	83	1.092	0.453	35.28	35.99
41	42	0.273	0.113	35.28	35.99	83	84	1.002	0.416	14	14.28
41	43	0.455	0.189	35.28	35.99	13	85	0.819	0.340	35.28	35.99

The same voltage and power bases used for the IEEE 34-node test system were considered in the IEEE 85-node test feeder. Note that the total apparent power losses for the peak load condition in this test feeder are approximately $316.12 + j198.60$ kVA [27].

4.3. PV Curve and Objective Function Parametrization

The evaluation of the proposed optimization approach uses as the PV generation curve a typical 24 h curve reported in [22] for the city of Medellín in Colombia. The generation and demand curves are depicted in Figure 4.

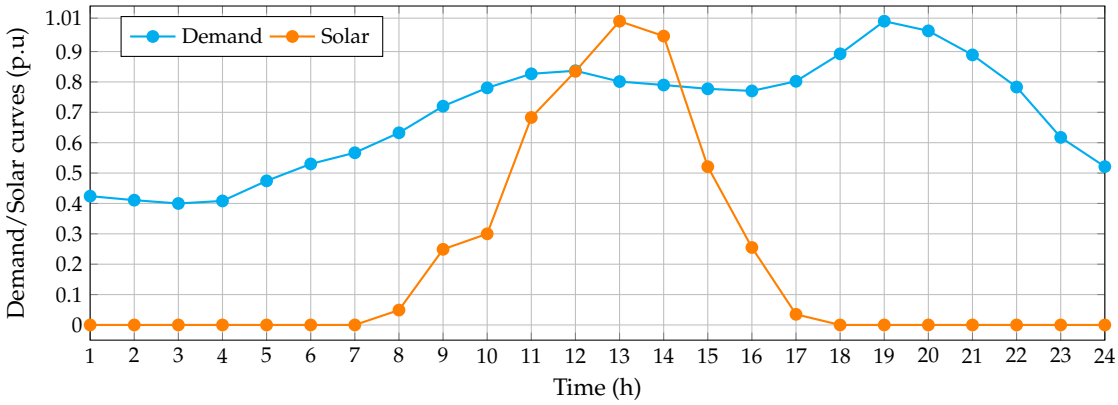

Figure 4. Solar generation and demand curves typical for the city of Medellín, Colombia.

The calculation of the objective function value was made by using the parameters reported in Table 3. Some of the parameters reported in this table were adapted from references [8,28], respectively.

Table 3. Parametrization of the objective and fitness functions.

Parameter	Value	Unit	Parameter	Value	Unit
C_{kWh}	0.1390	USD/kWh	T	365	days
t_a	10	%	t_e	2	%
N_t	20	years	Δh	1	h
C_{PV}	1036.49	USD/kWp	$C_{O\&M}$	0.0019	USD/kWh
$p_i^{pv,\max}$	2400	kW	$p_i^{pv,\min}$	0	kW
N_{pv}^{ava}	3	—	ΔV	±10	%
α_1	100×10^3	USD/V	α_2	100×10^3	USD/V
α_3	100×10^3	USD/W	—	—	—

In the case of the NMA, we considered a population with 10 individuals, 1000 iterations and 100 repetitions.

5. Numerical Validation and Discussion

To compare our proposed master–slave optimization approach based on the hybridization of the NMA with the successive approximation power flow method, we employed the GAMS software and the solver BONMIN to resolve the exact MINLP model (1)–(11) and a discrete–continuous version of the Chu and Beasley genetic algorithm (i.e., DCCBGA). The implementation of our proposed methods was in the MATLAB programming environment using own scripts. In the case of MATLAB implementations, its 2021*b* version was used on a PC with an AMD Ryzen 7 3700 2.3 GHz processor and 16.0 GB RAM, running on a 64-bit version of Microsoft Windows 10 single language. It is worth mentioning that to confirm that the GAMS and MATLAB models were complete equivalents, the benchmark cases were evaluated in both software, which provides the same operative costs when no PV sources are installed.

Note that Figure 5 illustrates the general implementation of the proposed NMA combined with the successive approximation power flow method in the MATLAB programming environment.

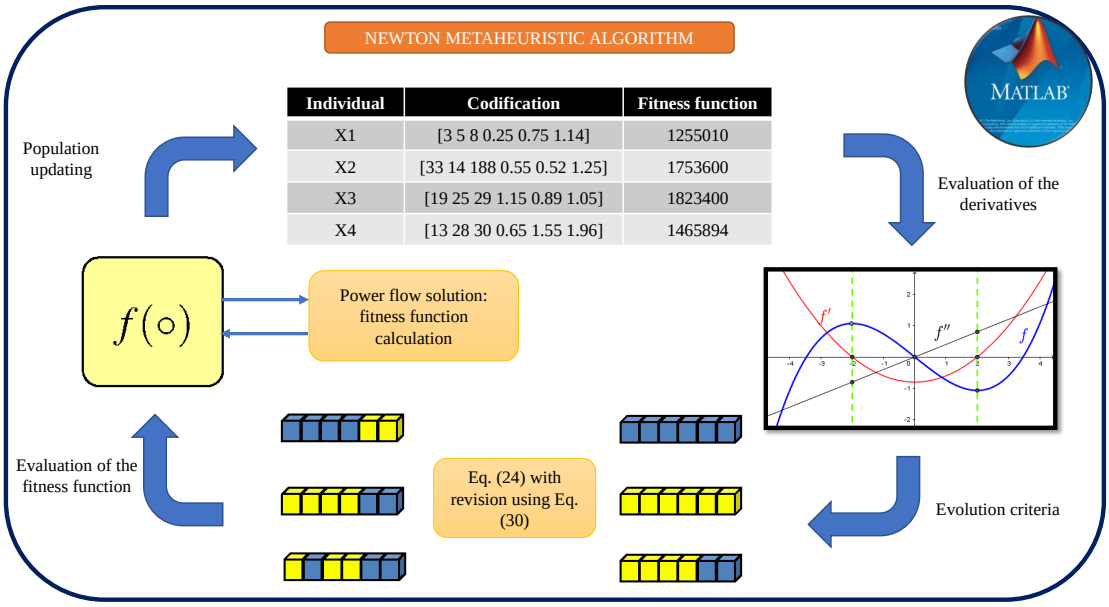

Figure 5. Implementation of the proposed methodology in the MATLAB programming environment.

In the general algorithm implementation presented in Figure 5, it is worth mentioning that all the system data are previously charged with the information of the test feeders as well as the generation and demand curves since these are input data that are required in the power flow solution and the algorithm evolution though the solution space (as can be seen in flow diagram in Figure 1).

5.1. Results in the IEEE 34-Node Test Feeder

Table 4 presents the numerical results provided by the BONMIN solver in the GAMS optimizer, the comparative DCCBGA, and the solution reached by the proposed NMA in the IEEE 34-node test feeder.

The numerical results in Table 4 show that: (i) the proposed NMA finds the best objective function value with an objective function value of USD 3,354,676.16/year which corresponds to a reduction of 26.89% with respect to the benchmark case, while the best solution reached by the DCCBGA is USD 35/year more expensive; (ii) the small differences between the solutions of the NMA and DCCBGA are mainly related to the nodes selected

for the location of the PV sources since nodes 10 and 24 in the NMA are replaced by neighborhood nodes 11 and 25 in the DCCBGA case; and (iii) the total power injections in the peak load cases are 4483.45 kW for the BONMIN solver, 4460.58 kW for the NMA, and 4460.52 kW for the NMA; this implies that with similar levels of power injections, the NMA finds a better set of nodes to locate all the generators owing to the objective function which is minimum for this algorithm when compared with the DCCBGA and the BONMIN solver, respectively.

Table 4. Optimal locations and sizes provided by the GAMS and the proposed approach in the IEEE 34-bus system.

Method	Site (Node)	Size (kW)	A^{cost} (USD/Year)	z_1 (USD/Year)	z_2 (USD/Year)
Bench. case	—	—	4,588,283.80	4,588,283.80	0
BONMIN	{26, 27, 34}	{2400, 747.45, 1336.00}	3,355,261.86	2,788,935.98	566,325.88
DCCBGA	{11, 23, 25}	{1055.54, 1347.95, 2057.09}	3,354,711.16	2,791,274.19	563,436.97
NMA	{10, 23, 24}	{994.25, 1409.42, 2056.85}	3,354,676.16	2,791,246.03	563,430.13

An important fact when the DCCBGA and the NMA are applied to solve the studied problem is that the former algorithm finds 11 solutions with the better objective function than the BONMIN solver, and the proposed NMA finds 12 additional solutions with better numerical performance with regard to the exact solver. This is particularly important since having multiple options for the location and sizing of the PV sources in the AC distribution network allows the utility to select the most adequate solution as a function of its grid needs and intervention possibilities.

To ensure that all the voltages are between their assigned regulation bounds, in Figure 6,the maximum and minimum voltage magnitudes experienced in the IEEE 34-node test feeder along the operation day are presented, where all the voltage magnitudes are contained in all the nodes of this AC grid.

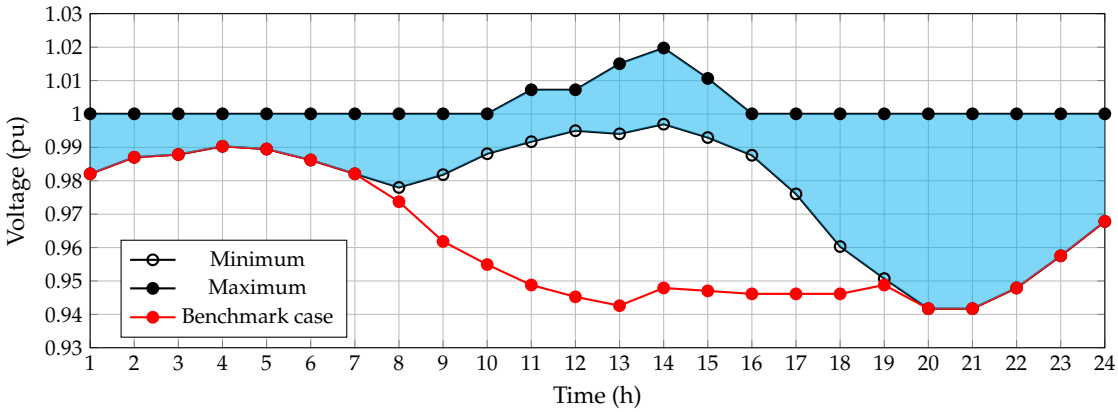

Figure 6. Minimum and maximum voltage magnitudes in the IEEE 34-node test feeder when the NMA solution is implemented.

The main result in Figure 6 is that for all the periods of time, all the voltages are between the assigned regulation bound, i.e., ±10%. In the worst case, hours 20 and 21, the active power injection in the PV sources is zero and the demand is maximum, the minimum voltage is 0.9417 pu; while in the period of time when the active power injections in the PV sources are maximum (hour 14), the maximum voltage in the grid has a magnitude of 1.0197 pu.

5.2. Results in the IEEE 85-Node Test Feeder

Table 4 presents best numerical results reached by the DCCBGA and the proposed NMA. It is worth mentioning that the BONMIN solvers do not converge to any solution for the IEEE 85-bus system.

The numerical results in Table 5 show that both algorithms present a very similar performance with respect to the final objective function value with a small difference of USD 48.02 per year of operation. In the case of the DCCBGA, 2594.03 kW of PV power are installed and the NMA installs 2598.44 KW of PV generation, i.e., a difference lower than 4.50 kW. However, the main difference lies in the nodes selected by each algorithm. These differences regarding nodes can be attributed to the fact that for the studied problem, the multi-period nature of the optimal power flow solution with PV sources can have multiple near-optimal solutions, i.e., different combinations of nodes with pretty similar objective function values.

Table 5. Optimal locations and sizes provided by the GAMS and the proposed approach in the IEEE 34-bus system.

Method	Site (Node)	Size (kW)	A^{Cost} (USD/Year)	z_1 (USD/Year)	z_2 (USD/Year)
Bench. case	—	—	2,686,114.05	2,686,114.05	0
DCCBGA	{47, 48, 68}	{260.33, 1165.68, 1168.02}	1,944,779.15	1,617,114.52	327,664.63
NMA	{35, 67, 71}	{1631.31, 463.33, 503.80}	1,944,731.13	1,616,509.04	328,222.09

On the other hand, Figure 7 presents the maximum and minimum voltage values for all the nodes in the IEEE 85-bus system for the solution provided by the NMA. Note that in the periods of time between 2020 and 2021 when the demand was maximum and the PV generation was zero, the voltage profiles of the network had a minimum of 0.87131 pu, which is a normal operative condition for this system [27] due to the fact that the only source in this period of time is the slack source.

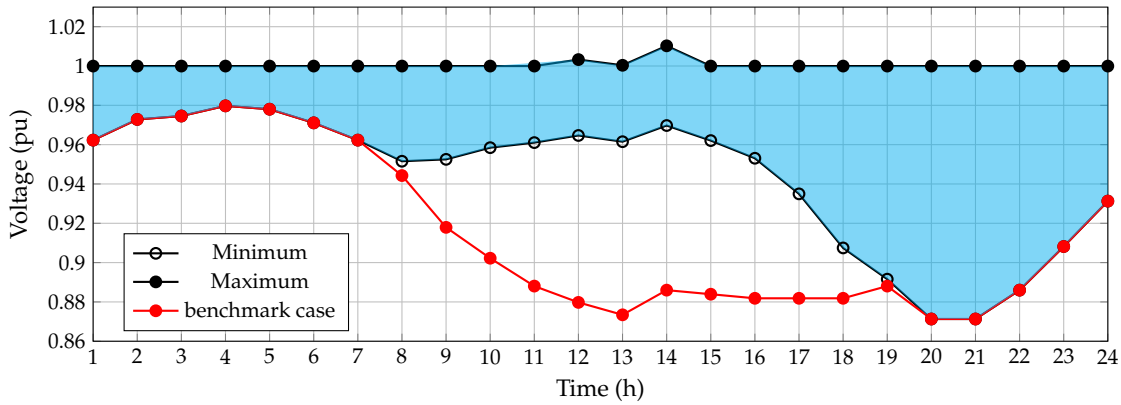

Figure 7. Minimum and maximum voltage magnitudes in the IEEE 85-node test feeder when the NMA solution is implemented.

Note that in the periods of time where the PV generation is prominent, i.e., 10 and 16 h, the voltage profile improves significantly, with respect to the benchmark voltage case; however, when no PV generation is available, the minimum voltage is equal to the benchmark case which is an expected behavior for this PV applications without batteries.

5.3. Additional Results

To observe the effect of the PV generation in the slack power source, we plotted the output power in the slack source for the benchmark case and the solution provided for the proposed NMA in both test feeders in Figure 8.

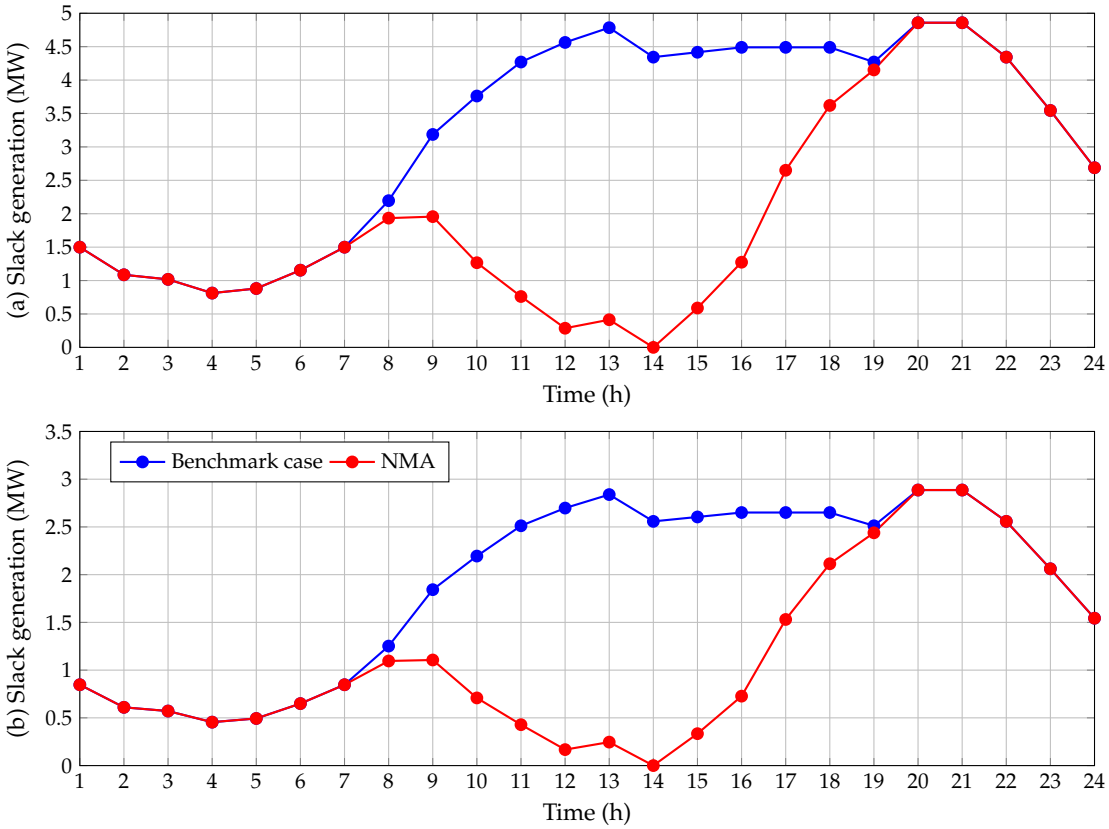

Figure 8. Slack generation output in the benchmark case and with the solution provided by the NMA: (**a**) IEEE 34-node test feeder; and (**b**) IEEE 85-bus system.

The behavior of the power generation as expected in the benchmark case follows the total power demand curves added to the terminals of the substation; however, when the PV generation was installed, we found the typical duck curve that decreases the power requirements in the slack node until zero when the PV generation is maximum. Note that the optimal solution provided by the NMA algorithm ensures that the total power in the slack source is always positive or zero, since our proposed model does not consider the possibility of selling energy to the sub-transmission system.

6. Conclusions and Future Works

The problem of the optimal sizing of PV sources in AC distribution networks was addressed in this research through the application of a master–slave optimization approach. In the master stage, the NMA was implemented which was entrusted to determine the nodes where the PV sources must be located and their corresponding sizes using discrete–continuous codification, where the discrete component was associated with the nodes and the continuous part with the assigned PV sizes; in the slave stage, each combination provided by the NMA was evaluated using the successive approximation power flow approach. Numerical results in the IEEE 34- and IEEE 85-bus systems demonstrated that the proposed NMA reaches better numerical results than the classical CBGA using the same codification and an exact solver in GAMS; in addition, for the IEEE 85-node test feeder, the exact approach with the BONMIN solver did not converge towards any feasible solution. The proposed NMA reaches reductions of approximately 26.89% and 27.60% regarding the benchmark cases for the IEEE 34- and IEEE 85-node test feeders. Differences with respect to the DCCBGA were less than USD 50 per year in both test feeders, even if these differences are small, these confirm that the proposed approach is better regarding the final objective function value with the main advantage that minimum parameters are required in its tuning when compared with the DCCBGA.

Even if the proposed optimization algorithm is general regarding the optimal sizing and location of the PV sources, an interesting research work that can be derived would be that of evaluating multiple PV generation curves—especially for countries (regions) that present high variations on the weather conditions as is the case of the four seasons. This will be an important analysis since the expected annual reductions in the total grid operational costs will be drastically reduced when PV generation availability becomes lower than 50% of their nominal capacities for long periods of time. Additional future works would be: (i) the application of the NMA to determine the optimal location and size of the distribution static compensators and capacitor banks in distribution networks; and (ii) the extension of the proposed algorithm to the simultaneous combination of renewable generation based on wind power and PV sources including reactive power compensation.

Author Contributions: Conceptualization, methodology, software, and writing—review and editing, O.D.M.; L.F.G.-N.; L.A.-B.; A.A.-L. and C.Á.-A. All authors have read and agreed to the published version of the manuscript.

Funding: This work was supported in part by the Centro de Investigación y Desarrollo Científico de la Universidad Distrital Francisco José de Caldas under grant 1643-12-2020 associated with the project: "Desarrollo de una metodología de optimización para la gestión óptima de recursos energéticos distribuidos en redes de distribución de energía eléctrica".

Institutional Review Board Statement: Not applicable.

Informed Consent Statement: Not applicable.

Data Availability Statement: No new data were created or analyzed in this study. Data sharing is not applicable to this article.

Acknowledgments: This research was partially supported by Minciencias, Instituto Tecnológico Metropolitano, Universidad Nacional de Colombia and Universidad del Valle, under the research project "Estrategias de dimensionamiento, planeación y gestión inteligente de energía a partir de la integración y la optimización de las fuentes no convencionales, los sistemas de almacenamiento y cargas eléctricas, que permitan la generación de soluciones energéticas confiables para los territorios urbanos y rurales de Colombia", which belongs to the research program "Estrategias para el desarrollo de sistemas energéticos sostenibles, confiables, eficientes y accesibles para el futuro de Colombia".

Conflicts of Interest: The authors declare no conflict of interest.

References

1. Montoya, O.D.; Serra, F.M.; Angelo, C.H.D. On the Efficiency in Electrical Networks with AC and DC Operation Technologies: A Comparative Study at the Distribution Stage. *Electronics* **2020**, *9*, 1352. [CrossRef]
2. Kien, L.C.; Nguyen, T.T.; Pham, T.D.; Nguyen, T.T. Cost reduction for energy loss and capacitor investment in radial distribution networks applying novel algorithms. *Neural Comput. Appl.* **2021**, *33*, 15495–15522. [CrossRef]
3. Celli, G.; Pilo, F.; Pisano, G.; Cicoria, R.; Iaria, A. Meshed vs. radial MV distribution network in presence of large amount of DG. In Proceedings of the IEEE PES Power Systems Conference and Exposition, New York, NY, USA, 10–13 October 2004. [CrossRef]
4. Zheng, X.; Yi, J.; Wang, Q. Research on Rural Distribution Network Reactive Power Dynamic Monitoring and Auto-Compensation System. In Proceedings of the 2017 2nd International Conference on Electrical, Control and Automation Engineering (ECAE 2017), Beijing, China, 24–25 December 2017. [CrossRef]
5. Salau, A.O.; Gebru, Y.W.; Bitew, D. Optimal network reconfiguration for power loss minimization and voltage profile enhancement in distribution systems. *Heliyon* **2020**, *6*, e04233. [CrossRef]
6. Montoya, O.D.; Gil-González, W.; Grisales-Noreña, L. An exact MINLP model for optimal location and sizing of DGs in distribution networks: A general algebraic modeling system approach. *Ain Shams Eng. J.* **2020**, *11*, 409–418. [CrossRef]
7. Kaur, S.; Kumbhar, G.; Sharma, J. A MINLP technique for optimal placement of multiple DG units in distribution systems. *Int. J. Electr. Power Energy Syst.* **2014**, *63*, 609–617. [CrossRef]
8. Wang, P.; Wang, W.; Xu, D. Optimal Sizing of Distributed Generations in DC Microgrids With Comprehensive Consideration of System Operation Modes and Operation Targets. *IEEE Access* **2018**, *6*, 31129–31140. [CrossRef]
9. Rajbongshi, R.; Borgohain, D.; Mahapatra, S. Optimization of PV-biomass-diesel and grid base hybrid energy systems for rural electrification by using HOMER. *Energy* **2017**, *126*, 461–474. [CrossRef]
10. Arévalo-Cordero, P.; Benavides, D.J.; Leonardo, J.; Hernández-Callejo, L.; Jurado, F. Optimal energy management strategies to reduce diesel consumption for a hybrid off-grid system. *Rev. Fac. Ing. Univ. Antioq.* **2020**, 47–58. [CrossRef]

11. Zafoschnig, L.A.; Nold, S.; Goldschmidt, J.C. The Race for Lowest Costs of Electricity Production: Techno-Economic Analysis of Silicon, Perovskite and Tandem Solar Cells. *IEEE J. Photovolt.* **2020**, *10*, 1632–1641. [CrossRef]
12. Zsiborács, H.; Baranyai, N.H.; Vincze, A.; Pintér, G. An Economic Analysis of the Shading Effects of Transmission Lines on Photovoltaic Power Plant Investment Decisions: A Case Study. *Sensors* **2021**, *21*, 4973. [CrossRef]
13. Paz-Rodríguez, A.; Castro-Ordoñez, J.F.; Montoya, O.D.; Giral-Ramírez, D.A. Optimal Integration of Photovoltaic Sources in Distribution Networks for Daily Energy Losses Minimization Using the Vortex Search Algorithm. *Appl. Sci.* **2021**, *11*, 4418. [CrossRef]
14. Gil-González, W.; Montoya, O.D.; Grisales-Noreña, L.F.; Perea-Moreno, A.J.; Hernandez-Escobedo, Q. Optimal Placement and Sizing of Wind Generators in AC Grids Considering Reactive Power Capability and Wind Speed Curves. *Sustainability* **2020**, *12*, 2983. [CrossRef]
15. Buitrago-Velandia, A.F.; Montoya, O.D.; Gil-González, W. Dynamic Reactive Power Compensation in Power Systems through the Optimal Siting and Sizing of Photovoltaic Sources. *Resources* **2021**, *10*, 47. [CrossRef]
16. Valencia, A.; Hincapie, R.A.; Gallego, R.A. Optimal location, selection, and operation of battery energy storage systems and renewable distributed generation in medium–low voltage distribution networks. *J. Energy Storage* **2021**, *34*, 102158. [CrossRef]
17. Jeong, S.; Kim, P. A Population-Based Optimization Method Using Newton Fractal. *Complexity* **2019**, *2019*, 5379301. [CrossRef]
18. Mosa, M.A.; Ali, A. Energy management system of low voltage dc microgrid using mixed-integer nonlinear programing and a global optimization technique. *Electr. Power Syst. Res.* **2021**, *192*, 106971. [CrossRef]
19. Molina, A.; Montoya, O.D.; Gil-González, W. Exact minimization of the energy losses and the CO_2 emissions in isolated DC distribution networks using PV sources. *Dyna* **2021**, *88*, 178–184. [CrossRef]
20. Bernal-Romero, D.L.; Montoya, O.D.; Arias-Londoño, A. Solution of the Optimal Reactive Power Flow Problem Using a Discrete-Continuous CBGA Implemented in the DigSILENT Programming Language. *Computers* **2021**, *10*, 151. [CrossRef]
21. Gholizadeh, S.; Danesh, M.; Gheyratmand, C. A new Newton metaheuristic algorithm for discrete performance-based design optimization of steel moment frames. *Comput. Struct.* **2020**, *234*, 106250. [CrossRef]
22. Grisales-Noreña, L.F.; Montoya, O.D.; Ramos-Paja, C.A. An energy management system for optimal operation of BSS in DC distributed generation environments based on a parallel PSO algorithm. *J. Energy Storage* **2020**, *29*, 101488. [CrossRef]
23. Montoya, O.D.; Gil-González, W. On the numerical analysis based on successive approximations for power flow problems in AC distribution systems. *Electr. Power Syst. Res.* **2020**, *187*, 106454. [CrossRef]
24. Herrera, M.C.; Montoya, O.D.; Molina-Cabrera, A.; Grisales-Noreña, L.F.; Giral-Ramirez, D.A. Convergence analysis of the triangular-based power flow method for AC distribution grids. *Int. J. Electr. Comput. Eng.* **2022**, *12*, 41. [CrossRef]
25. Montoya, O.D.; Molina-Cabrera, A.; Hernández, J.C. A Comparative Study on Power Flow Methods Applied to AC Distribution Networks with Single-Phase Representation. *Electronics* **2021**, *10*, 2573. [CrossRef]
26. Zhang, D.; Fu, Z.; Zhang, L. An improved TS algorithm for loss-minimum reconfiguration in large-scale distribution systems. *Electr. Power Syst. Res.* **2007**, *77*, 685–694. [CrossRef]
27. Prakash, D.; Lakshminarayana, C. Optimal siting of capacitors in radial distribution network using Whale Optimization Algorithm. *Alex. Eng. J.* **2017**, *56*, 499–509. [CrossRef]
28. Castiblanco-Pérez, C.M.; Toro-Rodríguez, D.E.; Montoya, O.D.; Giral-Ramírez, D.A. Optimal Placement and Sizing of D-STATCOM in Radial and Meshed Distribution Networks Using a Discrete-Continuous Version of the Genetic Algorithm. *Electronics* **2021**, *10*, 1452. [CrossRef]